Nonlytic viral spread enhanced by autophagy components

Sara Whitney Bird[a], Nathaniel D. Maynard[b], Markus W. Covert[b], and Karla Kirkegaard[a,1]

Departments of [a]Microbiology and Immunology and [b]Bioengineering, Stanford University School of Medicine, Stanford, CA 94305

Edited by Eckard Wimmer, Stony Brook University, Stony Brook, NY, and approved July 30, 2014 (received for review January 23, 2014)

The cell-to-cell spread of cytoplasmic constituents such as nonenveloped viruses and aggregated proteins is usually thought to require cell lysis. However, mechanisms of unconventional secretion have been described that bypass the secretory pathway for the extracellular delivery of cytoplasmic molecules. Components of the autophagy pathway, an intracellular recycling process, have been shown to play a role in the unconventional secretion of cytoplasmic signaling proteins. Poliovirus is a lytic virus, although a few examples of apparently nonlytic spread have been documented. Real demonstration of nonlytic spread for poliovirus or any other cytoplasmic constituent thought to exit cells via unconventional secretion requires demonstration that a small amount of cell lysis in the cellular population is not responsible for the release of cytosolic material. Here, we use quantitative time-lapse microscopy to show the spread of infectious cytoplasmic material between cells in the absence of lysis. siRNA-mediated depletion of autophagy protein LC3 reduced nonlytic intercellular viral transfer. Conversely, pharmacological stimulation of the autophagy pathway caused more rapid viral spread in tissue culture and greater pathogenicity in mice. Thus, the unconventional secretion of infectious material in the absence of cell lysis is enabled by components of the autophagy pathway. It is likely that other nonenveloped viruses also use this pathway for nonlytic intercellular spread to affect pathogenesis in infected hosts.

virus spread | live imaging

Viruses have traditionally been classified as "nonlytic" (capable of exiting host cells without killing them) and "lytic" (exiting the host cell with concomitant cell lysis). Enveloped viruses such as hepatitis C, SARS coronavirus, and HIV acquire their envelopes and envelope proteins by budding through the ER, Golgi, and plasma membranes, respectively (1–3). After these budding events, the viral particles are either in a luminal compartment from which they reach the extracellular milieu via the conventional cellular secretion pathway or released directly outside of the cell.

Nonenveloped viruses such as adenovirus, SV40, and picornaviruses assemble in nonlumenal compartments and would thus seem to have no exit pathway besides dismantling the host cell membrane. However, data consistent with nonlytic spread of such viruses (4, 5) and of other cytoplasmic aggregates continue to accumulate. Among picornaviruses, the spread of Theiler's virus from infected neurons to surrounding glial cells occurs even in *wlds* mice, whose neurons are highly refractory to destruction (6). Both coxsackievirus B3 and hepatitis A virus (HAV) can spread between cells in the presence of neutralizing antibodies (7, 8). In fact, it is generally thought that HAV is released nonlytically (reviewed in ref. 9). Recently, the existence of infectious HAV particles within extracellular vesicles has been observed and shown to be dependent on proteins ALIX and VPS4B of the multivesicular body (MVB) pathway and independent of TSG101 or HRS from the MVB pathway as well Beclin-1 of the autophagy pathway (8). Finally, the release of cytoplasmic aggregates of huntingtin protein provides a nonviral example of potentially nonlytic spread (10). Documentation that such events are truly nonlytic, however, requires rigorous demonstration that no cell lysis occurred.

Unconventional secretion, the release of cytoplasmic constituents without involvement of the Golgi apparatus or apparent lysis of the cell, can occur by several different mechanisms (reviewed in ref. 11). Nonvesicular routes include the direct exit of mammalian fibroblast growth factor 2 and yeast a-factor across the plasma membrane (12–14). Vesicle-mediated pathways of unconventional secretion include the release of cargo into the extracellular milieu from secretory lysosomes (15) or the budding of cytoplasmic constituents into the lumen of endosomal compartments using machinery from the endosomal complexes required for transport (ESCRT), from which they can subsequently be secreted as exosomes (reviewed in 16). Interestingly, a requirement for autophagy proteins (Atg 5, 7, 8, 11, and 12) was shown for the secretion of *Dictyostelium discoideum* and *Saccharomyces cerevisiae* sporulation pheromone (17, 18) and of mammalian IL-1β (19).

We have hypothesized (20, 21) that poliovirus infection can spread via a route that employs elements of the autophagy pathway and the double-membraned topology of virus-induced cytoplasmic vesicles. Similarities between the membranous vesicles induced during infection with poliovirus and cellular autophagosomes include their ultrastructure, with two lipid bilayers surrounding lumen that contains cytosolic contents (22–24), and the colocalization of lipidated LC3, late endosomal LAMP-1, and lysosomal cathepsin (25). As part of their maturation, poliovirus-induced vesicles, like autophagosomes, become degradative due to fusion with endosomes and lysosomes (25). For autophagosomes, the subsequent destruction of the inner membrane is known to allow the pooling of luminal and cytoplasmic contents. We have reported previously that, for

Significance

The cell-to-cell spread of viruses that are not surrounded by membranes was thought to occur only by destruction of the infected cell, as no obvious path for a cytoplasmic particle to penetrate the plasma membrane exists. Nonetheless, it is known that spread within tissues in human infections is not always accompanied by obvious cell death. Here we use quantitative single-cell analysis to show that poliovirus can spread to a neighboring cell prior to bursting and killing the originally infected cell. This type of spread is dependent on components of the autophagy pathway, a recycling pathway that is found in all eukaryotes. This finding identifies targets to block the spread of viruses and other toxic cytoplasmic assemblages.

Author contributions: S.W.B., N.D.M., M.W.C., and K.K. designed research; S.W.B., N.D.M., and K.K. performed research; N.D.M. and M.W.C. contributed new reagents/analytic tools; S.W.B., N.D.M., and K.K. analyzed data; and S.W.B. and K.K. wrote the paper.

The authors declare no conflict of interest.

This article is a PNAS Direct Submission.

Freely available online through the PNAS open access option.

[1]To whom correspondence should be addressed. Email: karlak@stanford.edu.

This article contains supporting information online at www.pnas.org/lookup/suppl/doi:10.1073/pnas.1401437111/-/DCSupplemental.

poliovirus, stimulation of autophagic processes by rapamycin increases both the intracellular yield and extracellular release of virus (20, 21). We proposed a mechanism by which viral release could be accomplished nonlytically: If an immature double-membraned vesicle that had entrapped virus-containing cytoplasm were to fuse with the plasma membrane, a membranous bleb that contained virus would be released. If the inner membrane had been degraded, the pooled luminal and cytoplasmic contents, including virus, would be released unbounded (Fig. 1*A*). We have termed this hypothesis "AWOL" (autophagosome-mediated exit without lysis) (21). However, it has been difficult to test this and other hypotheses concerning unconventional secretion because the use of cell populations makes it nearly impossible to exclude the possibility that lysis of a few cells is responsible for the release of cytoplasmic constituents (26). Here, we used live imaging of poliovirus-infected cells to show direct transfer of infection between living cells and a role for autophagic constituents in this nonlytic spread.

Results

Establishing a Real-Time, Single-Cell Assay for Poliovirus Spread. Mammalian protein LC3 becomes lipidated and membrane-associated upon induction of autophagy (27, 28) and during infection with several different picornaviruses, including poliovirus, rhinovirus, enterovirus 71, coxsackievirus B3, and foot-and-mouth disease virus (20, 29–32). To monitor the induction of autophagosome-like structures during the course of poliovirus infection, we used a human hepatocyte-derived cell line, Huh7-A-1 (33), that constitutively expresses GFP-LC3, in which GFP is fused to the C terminus of the autophagy protein LC3 (27, 28). GFP-LC3 fusions are frequently used to monitor the induction of autophagy; in the Huh7-A-1/GFP-LC3 cells used in the present study, the fusion protein was only slightly overexpressed with respect to endogenous LC3 and did not interfere with its lipidation (Fig. S1). Uninfected Huh7-A-1/GFP-LC3 cells and cells infected at a multiplicity of infection (MOI) of 0.1 plaque-forming units (PFU) per cell were monitored continuously by fluorescence microscopy in a heated CO_2-containing chamber. Time-lapse microscopy (Movie S1) showed that the percentage of GFP-LC3–expressing cells increased over time in the infected but not the uninfected cells (Fig. 1 *B* and *C*).

To determine whether the induction of GFP-LC3 puncta by poliovirus infection was cell-autonomous or not, we monitored the formation of autophagosome-like structures and poliovirus infection through multiple cycles of infection by time-lapse microscopy. To this end, we used an engineered poliovirus genome that expresses the fluorescent protein DsRed (PV-DsRed) fused to the C terminus of the nonstructural 2A protein (34). Thus, the virus particles themselves were not labeled, but the timing and location of infection of individual cells can be monitored upon accumulation of 2A-DsRed protein. PV-DsRed grows more slowly than wild-type virus but retains the inserted sequences through multiple cycles of infection (34). When GFP-LC3–expressing cells were infected with PV-DsRed at the low MOI of 0.1 PFU per cell, individual cells developed both GFP-LC3 and DsRed fluorescence with a similar time course (Fig. 1 *D* and *E* and Movie S2). Three waves of LC3 punctum formation were seen (Fig. 1*D*), followed by waves of DsRed fluorescence in the same cells until virtually all of the cells were infected. On average, the GFP-LC3 puncta appeared ∼4 h postinfection, 2.2 h before the first DsRed signal. The temporal displacement of the DsRed signal is most likely to result from the requirement for new synthesis of 2A-DsRed upon viral infection, whereas the GFP-LC3 signal preexists in the host cells. That infection and the formation of GFP-LC3 puncta occurred in the same cells through several rounds of infection argues that punctum formation is not induced by a secreted signal from neighboring infected cells.

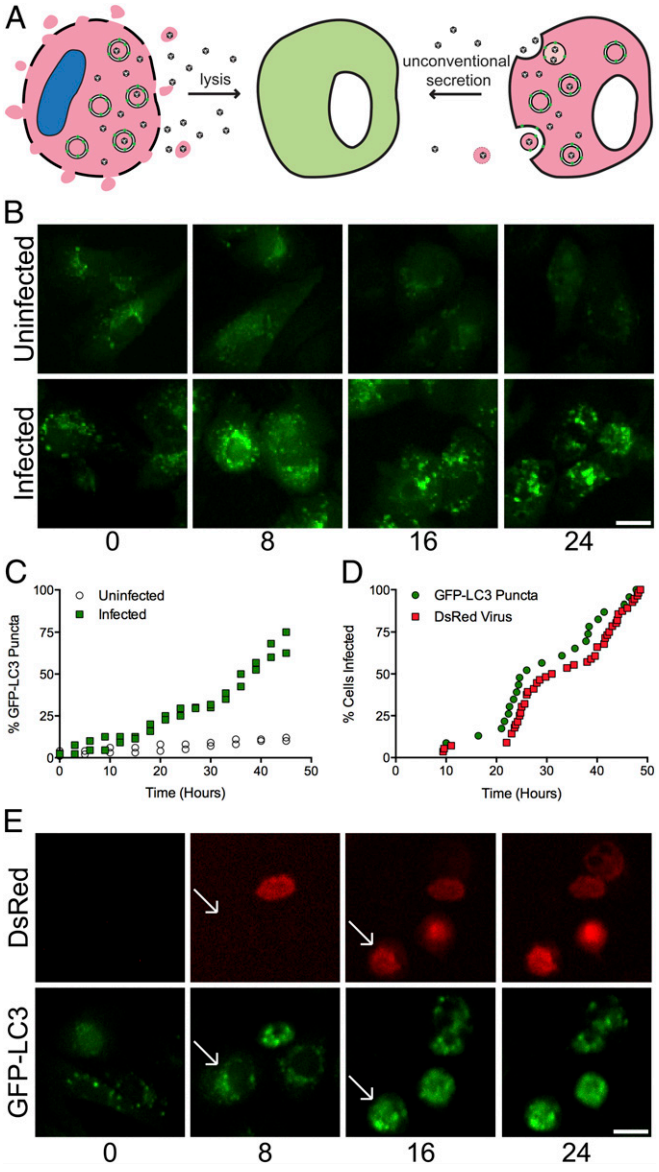

Fig. 1. Live-cell imaging of poliovirus-infected cells. (*A*) Proposed modes of spread for poliovirus. For most cell lines in tissue culture, lysis occurs 10–12 h after infection. The nonlytic route of viral spread proposed, a form of unconventional secretion, would result in the release of a few virus particles from a living cell, either from intact or ruptured inner compartments of autophagosome-like vesicles induced during infection. Pink cytoplasm indicates infection by PV-DsRed virus. The nucleus in the ruptured infected cell is blue, reflecting the use of the live-dead indicator in the experiments presented. The diffuse green in the uninfected cell represents the cytoplasmic form of GFP-LC3, whereas green puncta indicate the lipidation and membrane localization of GFP-LC3 in infected cells. (*B*) Single-cell images from Movie S1 of Huh7-A-1/GFP-LC3 cells infected with 2A-144-DsRed poliovirus (PV-DsRed) at a multiplicity of infection (MOI) of 0.1 PFU per cell and imaged every 12 min for 48 h, comparing GFP-LC3 puncta in uninfected (*Upper*) and infected (*Lower*). (*C*) Quantification of time-lapse imaging showing the percentage of cells with GFP-LC3 puncta over 48 h. For each time point, ∼100 cells were scored; data from two replicates are shown. (*D*) Time course data from one movie showing the percent of infected cells over time. Formation of GFP-LC3 puncta coincided with DsRed expression. (Scale bars: 25 μm.) $^{****}P < 0.0001$. (*E*) Single-cell images of Huh7-A-1/GFP-LC3 cells over 24 h of infection, showing both DsRed expression (*Upper*) and GFP-LC3 distribution (*Lower*). Arrows identify individual cells as GFP-LC3 puncta develop and viral infection progresses.

Stimulating the Autophagy Pathway Increases Poliovirus Spread in Tissue Culture. We have previously shown that stimulation of autophagy by rapamycin increases the extracellular yield of poliovirus (20). Cell exit is, however, only part of viral spread. To determine how the cellular autophagy pathway or its components affect multiple cycles of cell-to-cell spread, we used pharmacological agents known to stimulate autophagy that could be used over the 48-h time course of live microscopy experiments and in mouse models. Loperamide and nicardipine are both FDA-approved Ca^{2+} channel blockers, prescribed for diarrhea and heart arrhythmias, respectively. Both drugs inhibit calpains, thus stimulating autophagy and increasing the abundance of its components (35). Although other side effects are possible, nicardipine and loperamide have advantages over rapamycin because they do not inhibit protein translation or affect the cell cycle.

The effect of loperamide and nicardipine on viral spread was monitored over 48 h in tissue culture by fluorescence microscopy (Fig. 2 *A*–*C* and Movies S3–S5). As infection progressed, the cell-to-cell spread of poliovirus infection proceeded more rapidly in the presence of either loperamide (Fig. 2*B*) or nicardipine (Fig. 2*C*). The presence of loperamide or nicardipine had no detectable effect on viral protein synthesis in cells infected in the presence of guanidine, which inhibits RNA synthesis, making the input RNA was the sole template (Fig. S2*A*). These compounds also did not affect the accumulation of intracellular RNA (Fig. S2*B*). Therefore, neither loperamide nor nicardipine affected viral cell entry, translation, or RNA accumulation.

Stimulating the Autophagy Pathway Increases Poliovirus Pathogenesis. To observe the effect of autophagy stimulation in a mouse model of human poliovirus infection, we tested viral growth and pathogenesis in cPVR mice, which are ICR mice transgenic for the human poliovirus receptor (CD155) under the control of the murine actin promoter (36). When mice were treated with the autophagy stimulator loperamide, higher levels of LC3-II were observed in the calf muscle (Fig. 2*D*). The presence of loperamide greatly increased the rate of paralysis (Fig. 2*E*). It also greatly increased the yield of poliovirus found in the mouse calf muscle

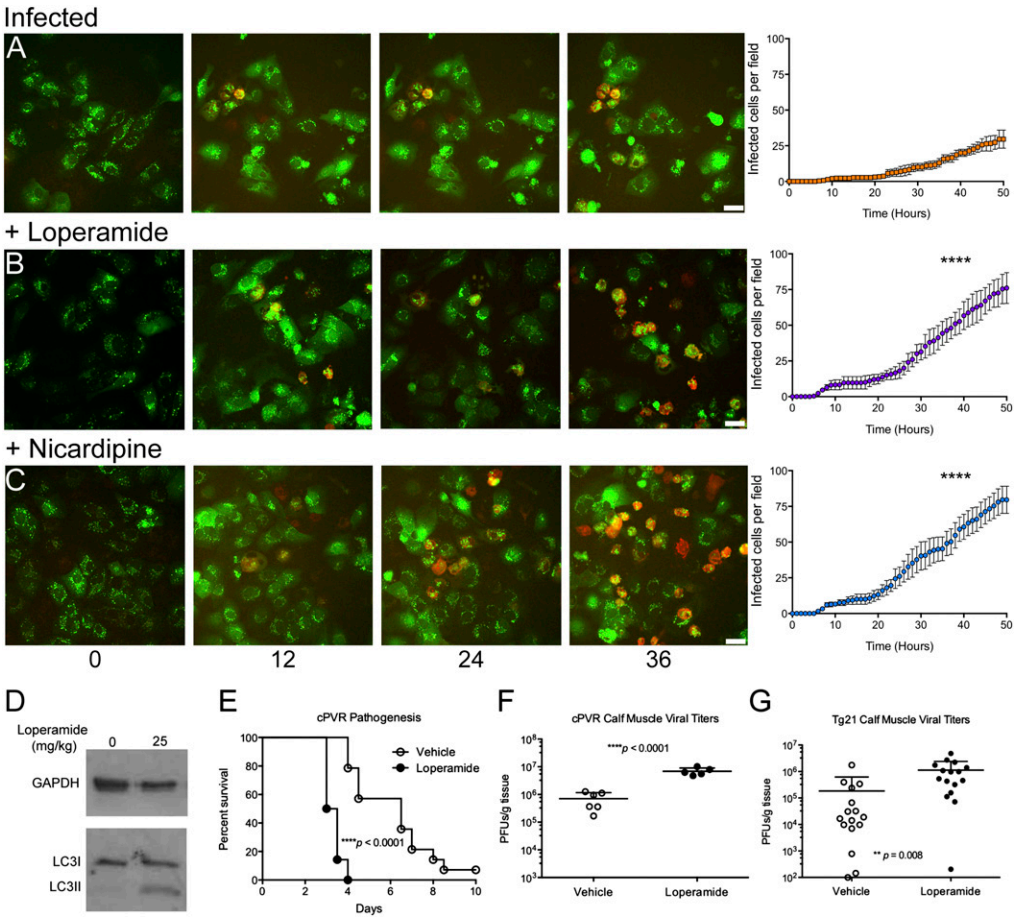

Fig. 2. Stimulation of the autophagy pathway increases the rate of viral spread and pathogenesis. Huh7-A-1/GFP-LC3 cells were infected with PV-DsRed at a MOI of 0.1 PFU per cell and imaged every 12 min for 48 h. Analysis of single-cell images yielded time courses of infection (*Right*) for untreated cells (*A*) and for cells treated with either 5 μM loperamide (*B*) or 5 μM nicardipine (*C*); see Movies S3, S4, and S5, respectively. (Scale bars: 25 μm.) Mean and SE are shown from three movies for each condition. Statistical significance determined by linear regression analysis comparing slopes of drug-treated to control group. ****$P < 0.0001$. (*D*) cPVR mice, which express the human poliovirus receptor in an ICR background, were inoculated intramuscularly with 5×10^6 PFU of Type 1 Mahoney virus. Mice (14 per condition) were treated every 12 h with 25 mg/kg loperamide, or with a control solution, by i.p. injection. LC3 and control proteins from gastrocnemius tissue were displayed by SDS/PAGE and visualized by immunoblotting. Bands for the GAPDH loading control, LC3I and LC3II, the unlipidated and lipidated protein species, are identified. (*E*) The time of onset of paralysis of cPVR mice was monitored. Statistical significance was determined using the log-rank test. (*F*) The titers of poliovirus in inoculated calf muscles of cPVR mice were determined 4 d after infection. (*G*) Viral titers in the inoculated calf muscles of Tg21 mice, which express the poliovirus receptor in a C57BL/6 background and show greater susceptibility to poliovirus growth and pathogenesis than cPVR mice, were determined four days after infection with 3×10^5 PFU of virus. Statistical significance for *F* and *G* was determined using Student *t* test. Bars represent mean and SE.

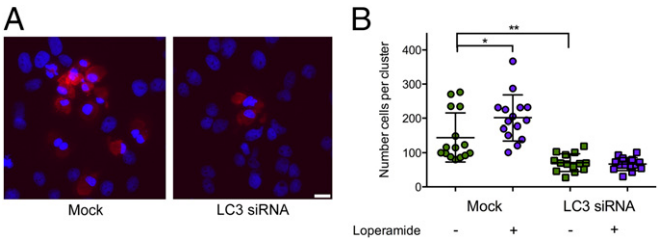

Fig. 3. Inhibition of LC3 expression reduces spread of poliovirus. (*A*) Huh7-A-1 cells treated for 48 h with control (luciferase) or LC3 siRNAs were infected with PV-DsRed at a MOI of 0.1 PFU per cell and for 24 h. Representative images of fluorescent, infected cells and the nuclei of all cells, revealed by DAPI staining are shown. (Scale bar: 25 μm.) (*B*) Numbers of infected cells in 15 randomly chosen plaques from control and LC3 siRNA-treated cells, with and without 5 μM loperamide 36 h postinfection. Statistical significance was determined using Student *t* test. $n = 15$. $^*P < 0.05$; $^{**}P < 0.01$.

harvested 4 d after inoculation in either the cPVR mice or in Tg21 mice, which express human CD155 under the control of the endogenous human promoter (Fig. 2 *F* and *G*; ref. 37). Rapid paralysis following intramuscular inoculation has three parts: viral growth in the inoculated muscle, axonal traffic from the infected muscle tissue to the CNS, and the infection and death of motor neurons in the CNS (38). Increased poliovirus pathogenesis by an autophagy stimulator argues that the autophagy pathway or its components stimulate viral growth, spread, or both in murine tissues.

Inhibition of Autophagy Reduces Poliovirus Spread in Tissue Culture. The few autophagy inhibitors that are currently available are limited for use in long-term experiments and in animals by their toxicity (39). In the present study, we used pools of siRNA that target both isoforms of the critical autophagy protein LC3 (20) and the extent of LC3 depletion was determined by immunoblotting (Fig. S3). To ask directly about the effect of LC3 depletion on viral spread through several cycles of infection, we used immunofluorescence to count the number of individual cells in infected clusters formed in control and LC3-depleted cultures after 24 h (Fig. 3*A*) or 36 h (Fig. 3*B*). LC3 depletion caused a significant decrease in the numbers of cells in randomly chosen clusters, and loperamide increased plaque size under these conditions. To test whether the enhancement of poliovirus spread by loperamide is due to its effects on the autophagy pathway, we tested the effect of loperamide on cells depleted of LC3. No loperamide effect was observed upon LC3 knockdown (Fig. 3*B*), consistent with the idea that loperamide stimulates poliovirus spread via its effect on the autophagy pathway or its components.

Single Cell Analysis Identifies Nonlytic Spread Events. We have established that stimulators of autophagic processes enhance the spread of poliovirus and autophagy inhibitors reduce viral spread, and have proposed a model by which autophagosome-like membranes provide a topological mechanism for the nonlytic release of cytoplasm (Fig. 1). However, we have not yet tested whether viral infection actually spreads without killing the original infected cells. In fact, this has been difficult to establish for most reports of unconventional secretion, because the amounts of extracellular secretory material are often so small that they could have been produced via lysis of only a few cells in the culture (26).

To determine whether poliovirus can spread nonlytically, we monitored viral transfer and cell viability simultaneously at the single-cell level. Cell viability during a 48-h time course was imaged by using both differential interference contrast (DIC) microscopy to monitor membrane integrity, and by the fluorescence of SYTOX Blue (Life Technologies), a cell-impermeable dye that binds quickly and with high affinity to nucleic acids when the cell membrane is compromised (Movie S6). Infection of both "donor" and "target" cells was monitored by the appearance of DsRed fluorescence. Then, we could ask whether target cells were infected before the adjacent donor cell lost its integrity. This was quite a stringent test, because DsRed fluorescence takes at least 5 h to develop after initial infection (Fig. 1; ref. 34).

Time-lapse fluorescence microscopy revealed the time courses of many individual cells following infection of an Huh7-A-1 monolayer at a very low multiplicity of infection (Fig. 4 and Movie S5). When viewed as single cells, the identification of donor and target cell pairs was unambiguous due to the low multiplicity of infection and the use of an agar overlay to limit long-range viral spread (Fig. 4*A*). When viewed as a population, cells infected by PV-DsRed in the first infectious cycle showed red fluorescence beginning at an average of 10 h postinfection, SYTOX Blue staining beginning at an average of 15 h postinfection, and membrane rupture by DIC microscopy beginning at 16 h postinfection (Fig. 4*B*).

The relative timing of death of the donor cell and detectable infection of the target cell (Δt) was quantified for individual cell pairs by setting the time of DsRed fluorescence in the target to zero and then subtracting the time of death of the donor. For most infectious events, Δt was a positive number; target cells lysed before detectable infection of their neighbors was observed.

However, negative values of Δt were also observed. The cell pair shown in Fig. 4*A*, for example, shows a previously infected donor cell infecting its target neighbor cell at 10 h after the

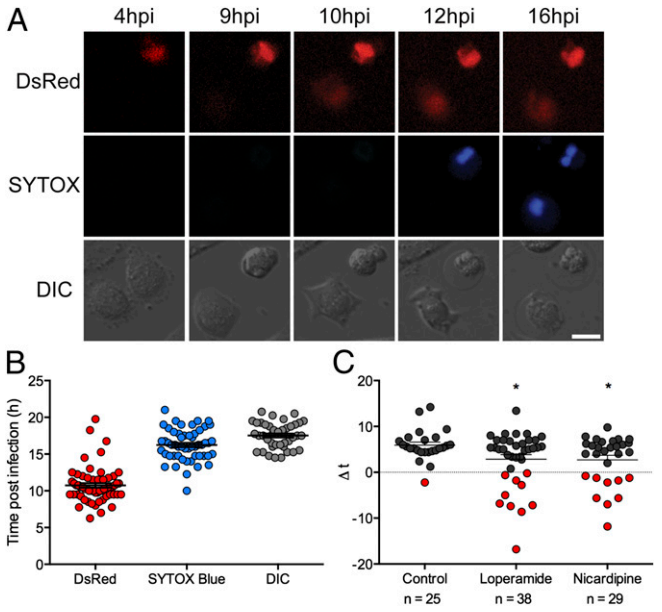

Fig. 4. Single-cell analysis of cell viability reveals nonlytic spread of poliovirus infection. Huh7-A-1 cells were inoculated with PV-DsRed at a MOI of 0.1 PFU per cell and imaged every 15 min for 24 h. SYTOX Blue (100 μM) was used to identify dead cells. (*A*) Single cell images taken from Movie S7 track the onset of the DsRed fluorescence that indicates viral infection (*Top*), the SYTOX staining that monitors cell death (*Middle*), and the DIC images that identify all cells and visualize the onset of membrane rupture (*Bottom*). (Scale bars: 25 μm.) (*B*) The times of initial signals for DsRed fluorescence, SYTOX fluorescence, or ruffling membranes in the DIC channel are plotted. Means are indicated, and error bars are SEM values. (*C*) Time difference (Δt) between the onset of DsRed signal in target cell and DIC membrane ruffling signal in donor cell for multiple donor and target pairs. Although mean values are indicated, data points shown as red circles fell outside the 95% range of a normal distribution of Δt using Fisher's exact test. All such events displayed negative values for Δt. $^*P < 0.05$ for each treatment.

experiment was initiated. However, SYTOX blue staining and DIC imaging revealed that the donor cell maintained its membrane integrity for 12 h. This event thus had a Δt value of −2 h and is a clear example of functional nonlytic viral spread, documented here, to our knowledge, for the first time.

Stimulating Autophagy Increases Frequency of Nonlytic Spread Events. To inquire whether stimulation of the autophagy pathway affected nonlytic viral spread, we screened single cells that were infected with PV-DsRed in the absence or presence of loperamide or nicardipine and determined the values of Δt for well isolated cells in randomly chosen fields. When cells were exposed to the autophagy-stimulating compounds, there was a significant increase in the number of infectious events that fell outside a normal distribution of Δt, all of which showed negative values (Fig. 4*C*). Thus, components of the autophagy pathway or the process itself increased the frequency of these unambiguous cases of nonlytic viral spread.

Discussion

Traditionally, only enveloped viruses were thought to have the correct topology to exit a cell without lysing it. Nonetheless, there have been numerous reports of cytoplasmic assemblages, including nonenveloped viruses and pathogenic aggregated proteins, that are found in the extracellular milieu with no apparent lysis of the donor cell population. However, it has been difficult to prove that the small amount of extracellular material did not result from the lysis or extravasation of a few cells. Here, using time-lapse microscopy of individual cells infected with poliovirus, we have visualized and documented infectious spread of a nonenveloped virus between living cells.

Although poliovirus infection is highly lytic in most cells in tissue culture, and paralytic poliomyelitis in vivo is caused by the destruction of neurons in the CNS, little is known about the mechanisms of poliovirus spread via the intestine, Peyer's patches, bloodstream, muscle tissue, and peripheral neurons in a natural infection. Therefore, a role for nonlytic spread in poliovirus propagation and transmission is, at this point, a matter of speculation. However, it has been demonstrated here that poliovirus can spread without cell lysis, and this is likely to be a property of other nonenveloped viruses, such as hepatitis A, as well. We argue that the analysis of individual cells can be used to document nonlytic spread of cytoplasmic constituents unambiguously.

What is the mechanism of nonlytic viral spread? That its incidence increased upon treatment with loperamide or nicardipine (Fig. 4*C*) and that the reduction of LC3 abundance by RNAi treatment reduces both viral spread and its enhancement by loperamide (Fig. 3*B*) argue that induction of the autophagy pathway facilitates nonlytic spread. The presence of extracellular virus early in poliovirus infection is dependent upon autophagy proteins ATG12 and LC3 (20). However, it is insensitive to treatment with spautin-1 (39, 40), an inhibitor of the autophagy pathway that causes the destabilization of beclin-1 protein, which acts to nucleate the assembly of the preautophagosomal membrane. Therefore, it is likely that poliovirus intercepts the autophagy pathway downstream of beclin-1, using components such as ATG12 and LC3 that are required to build double-membraned vesicles. Viral components 2BC and 3A are sufficient to induce double-membraned vesicles (24), with viral protein 2BC being sufficient to recruit LC3 to membranes (41). As shown in Fig. 1*A*, fusion of a double-membraned vesicle with the plasma membrane should release an exosome-like vesicle. If such a vesicle contains an intact poliovirion, fuses with a neighboring cell, and releases the virion into the cytoplasm, it is not likely to initiate a productive infection because virion binding to the poliovirus receptor is required for RNA release (42). Therefore, for viral spread to occur, the exosome-like vesicle would need to be unstable or contain infectious RNA.

Membrane-wrapped HAV particles have been observed and likened to exosomes (8). Their formation was shown to be dependent on some, but not all, components of the MVB pathway, and, like the early exit of poliovirus, not on beclin-1. Interestingly, the unconventional secretion of *S. cerevisiae* and *D. discoideum* Acb1 requires participation of proteins from both the canonical autophagy and MVB pathways, raising the possibility that these pathways are not so distinct after all (17, 18). "Exosomal" fractions are preparations of extracellular vesicles isolated by differential sedimentation; they are often assumed to derive exclusively from the ESCRT pathway. FACS analysis, however, has revealed great heterogeneity in such populations, with vesicles that bear markers of the MVB, autophagy, and mitochondrial pathways (43). As with poliovirus, the infectious mechanism of the membrane-wrapped HAV particles is currently being investigated.

The complex pathway of cellular autophagy, with its dependence on nutritional signals, predilection for interconverting cellular topologies, and ability to accomplish unconventional secretion of cytoplasmic contents, is proving to be a playground for those microbes sufficiently well evolved to avoid and subvert it. Autophagy and other mechanisms of cytoplasmic transfer between living cells are likely to provide targets for halting the spread of toxic assemblages and for modulating cell-to-cell communication.

Materials and Methods

Detailed experimental information is provided in *SI Materials and Methods*.

Time-Lapse Microscopy. Huh7-A-1/GFP-LC3 cells were seeded at 10,000 cells per well in optical-bottom 96-well plates coated in 5μg/mL fibronectin (Nunc) and incubated overnight at 37 °C. Cells were washed once with PBS supplemented with $MgCl_2$ and $CaCl_2$ (PBS^+), followed by inoculation with PV-DsRed at a low multiplicity of infection (≤0.1 PFU per cell). Adsorption proceeded for 30 min at 37 °C, after which the inoculum was removed and the cells washed with PBS^+ three times. A 1:1 DMEM:agarose overlay supplemented with 5% (vol/vol) FBS was added to preclude long-distance viral spread. Autophagy stimulators or DMSO were added directly. Cells were placed on a heated stage with 5% (vol/vol) CO_2 and imaged every 12–15 min for 24–48 h using a Nikon Eclipse Ti inverted microscope (20× objective). For SYTOX experiments, Huh7-A-1 cells were seeded as described in *SI Materials and Methods*. Following inoculation with PV-DsRed, 25 μL of 100 nM SYTOX Blue (Life Technologies) was added to the overlay and images taken every 15 min for 24 h.

Analysis. Analysis of time-lapse movies was done in MatLab using a custom graphical user interface as well as ImageJ. Statistical analyses were done using Prism software (Graphpad Software). Statistical significance was determined using linear regression to compare slopes, the Student *t* test to compare means, the Fisher's exact test for categorical data, and the log-rank test for survival curves.

ACKNOWLEDGMENTS. We thank Roberto Mateo, Andres Tellez, Timothy Lee, Eileen, Clancy, and Julie Theriot for helpful discussions and Peter Sarnow for careful reading of the manuscript. This work was supported by a BioX Interdisciplinary Initiatives Program Seed Grant (to M.W.C. and K.K.), National Institutes of Health (NIH) Training Grant T32 GM007276 (to S.W.B.), and NIH Grant R56 AI103500 (to K.K.).

1. Romero-Brey I, et al. (2012) Three-dimensional architecture and biogenesis of membrane structures associated with hepatitis C virus replication. *PLoS Pathog* 8(12):e1003056.
2. Cohen JR, Lin LD, Machamer CE (2011) Identification of a Golgi complex-targeting signal in the cytoplasmic tail of the severe acute respiratory syndrome coronavirus envelope protein. *J Virol* 85(12):5794–5803.
3. Votteler J, Sundquist WI (2013) Virus budding and the ESCRT pathway. *Cell Host Microbe* 14(3):232–241.
4. Lloyd RE, Bovee M (1993) Persistent infection of human erythroblastoid cells by poliovirus. *Virology* 194(1):200–209.
5. Pelletier I, Duncan G, Colbère-Garapin F (1998) One amino acid change on the capsid surface of poliovirus sabin 1 allows the establishment of persistent infections in HEp-2c cell cultures. *Virology* 241(1):1–13.
6. Roussarie JP, Ruffié C, Edgar JM, Griffiths I, Brahic M (2007) Axon myelin transfer of a non-enveloped virus. *PLoS ONE* 2(12):e1331.

7. Paloheimo O, et al. (2011) Coxsackievirus B3-induced cellular protrusions: Structural characteristics and functional competence. *J Virol* 85(13):6714–6724.
8. Feng Z, et al. (2013) A pathogenic picornavirus acquires an envelope by hijacking cellular membranes. *Nature* 496(7445):367–371.
9. Lemon SM (1985) Type A viral hepatitis. New developments in an old disease. *N Engl J Med* 313(17):1059–1067.
10. Ren PH, et al. (2009) Cytoplasmic penetration and persistent infection of mammalian cells by polyglutamine aggregates. *Nat Cell Biol* 11(2):219–225.
11. Nickel W (2010) Pathways of unconventional protein secretion. *Curr Opin Biotechnol* 21(5):621–626.
12. Steringer JP, et al. (2012) Phosphatidylinositol 4,5-bisphosphate (PI(4,5)P2)-dependent oligomerization of fibroblast growth factor 2 (FGF2) triggers the formation of a lipidic membrane pore implicated in unconventional secretion. *J Biol Chem* 287(33): 27659–27669.
13. Temmerman K, et al. (2008) A direct role for phosphatidylinositol-4,5-bisphosphate in unconventional secretion of fibroblast growth factor 2. *Traffic* 9(7):1204–1217.
14. Kuchler K, Sterne RE, Thorner J (1989) *Saccharomyces cerevisiae* STE6 gene product: A novel pathway for protein export in eukaryotic cells. *EMBO J* 8(13):3973–3984.
15. Rodríguez A, Webster P, Ortego J, Andrews NW (1997) Lysosomes behave as Ca2+-regulated exocytic vesicles in fibroblasts and epithelial cells. *J Cell Biol* 137(1):93–104.
16. Bissig C, Gruenberg J (2014) ALIX and the multivesicular endosome: ALIX in Wonderland. *Trends Cell Biol* 24(1):19–25.
17. Duran JM, Anjard C, Stefan C, Loomis WF, Malhotra V (2010) Unconventional secretion of Acb1 is mediated by autophagosomes. *J Cell Biol* 188(4):527–536.
18. Manjithaya R, Anjard C, Loomis WF, Subramani S (2010) Unconventional secretion of *Pichia pastoris* Acb1 is dependent on GRASP protein, peroxisomal functions, and autophagosome formation. *J Cell Biol* 188(4):537–546.
19. Dupont N, et al. (2011) Autophagy-based unconventional secretory pathway for extracellular delivery of IL-1β. *EMBO J* 30(23):4701–4711.
20. Jackson WT, et al. (2005) Subversion of cellular autophagosomal machinery by RNA viruses. *PLoS Biol* 3(5):e156.
21. Taylor MP, Burgon TB, Kirkegaard K, Jackson WT (2009) Role of microtubules in extracellular release of poliovirus. *J Virol* 83(13):6599–6609.
22. Dales S, Eggers HJ, Tamm I, Palade GE (1965) Electron Microscopic Study of the Formation of Poliovirus. *Virology* 26:379–389.
23. Schlegel A, Giddings TH, Jr, Ladinsky MS, Kirkegaard K (1996) Cellular origin and ultrastructure of membranes induced during poliovirus infection. *J Virol* 70(10): 6576–6588.
24. Suhy DA, Giddings TH, Jr, Kirkegaard K (2000) Remodeling the endoplasmic reticulum by poliovirus infection and by individual viral proteins: An autophagy-like origin for virus-induced vesicles. *J Virol* 74(19):8953–8965.
25. Richards AL, Jackson WT (2012) Intracellular vesicle acidification promotes maturation of infectious poliovirus particles. *PLoS Pathog* 8(11):e1003046.
26. Zhang M, Schekman R (2013) Cell biology. Unconventional secretion, unconventional solutions. *Science* 340(6132):559–561.
27. Kabeya Y, et al. (2000) LC3, a mammalian homologue of yeast Apg8p, is localized in autophagosome membranes after processing. *EMBO J* 19(21):5720–5728.
28. Ichimura Y, et al. (2000) A ubiquitin-like system mediates protein lipidation. *Nature* 408(6811):488–492.
29. O'Donnell V, et al. (2011) Foot-and-mouth disease virus utilizes an autophagic pathway during viral replication. *Virology* 410(1):142–150.
30. Huang SC, Chang CL, Wang PS, Tsai Y, Liu HS (2009) Enterovirus 71-induced autophagy detected in vitro and in vivo promotes viral replication. *J Med Virol* 81(7): 1241–1252.
31. Klein KA, Jackson WT (2011) Human rhinovirus 2 induces the autophagic pathway and replicates more efficiently in autophagic cells. *J Virol* 85(18):9651–9654.
32. Kemball CC, et al. (2010) Coxsackievirus infection induces autophagy-like vesicles and megaphagosomes in pancreatic acinar cells in vivo. *J Virol* 84(23):12110–12124.
33. Konduru K, Kaplan GG (2006) Stable growth of wild-type hepatitis A virus in cell culture. *J Virol* 80(3):1352–1360.
34. Teterina NL, Levenson EA, Ehrenfeld E (2010) Viable polioviruses that encode 2A proteins with fluorescent protein tags. *J Virol* 84(3):1477–1488.
35. Zhang L, et al. (2007) Small molecule regulators of autophagy identified by an image-based high-throughput screen. *Proc Natl Acad Sci USA* 104(48):19023–19028.
36. Crotty S, Hix L, Sigal LJ, Andino R (2002) Poliovirus pathogenesis in a new poliovirus receptor transgenic mouse model: Age-dependent paralysis and a mucosal route of infection. *J Gen Virol* 83(Pt 7):1707–1720.
37. Ida-Hosonuma M, et al. (2005) The alpha/beta interferon response controls tissue tropism and pathogenicity of poliovirus. *J Virol* 79(7):4460–4469.
38. Racaniello VR (2006) One hundred years of poliovirus pathogenesis. *Virology* 344(1): 9–16.
39. Liu J, et al. (2011) Beclin1 controls the levels of p53 by regulating the deubiquitination activity of USP10 and USP13. *Cell* 147(1):223–234.
40. Mateo R, et al. (2013) Inhibition of cellular autophagy deranges dengue virion maturation. *J Virol* 87(3):1312–1321.
41. Taylor MP, Kirkegaard K (2007) Modification of cellular autophagy protein LC3 by poliovirus. *J Virol* 81(22):12543–12553.
42. Mason PW, et al. (1993) Antibody-complexed foot-and-mouth disease virus, but not poliovirus, can infect normally insusceptible cells via the Fc receptor. *Virology* 192(2): 568–577.
43. Pallet N, et al. (2013) A comprehensive characterization of membrane vesicles released by autophagic human endothelial cells. *Proteomics* 13(7):1108–1120.